Hindawi Publishing Corporation
Mathematical Problems in Engineering
Volume 2013, Article ID 141849, 15 pages
http://dx.doi.org/10.1155/2013/141849

Research Article

A Novel Machine Learning Based Method of Combined Dynamic Environment Prediction

Wentao Mao,[1,2] Guirong Yan,[2] and Longlei Dong[2]

[1] *College of Computer and Information Engineering, Henan Normal University, Xinxiang 453007, China*
[2] *State Key Laboratory for Strength and Vibration, Xi'an Jiaotong University, Xi'an 710049, China*

Correspondence should be addressed to Wentao Mao; maowt.mail@gmail.com

Received 8 February 2013; Revised 9 May 2013; Accepted 10 May 2013

Academic Editor: Jun Zhao

In practical engineerings, structures are often excited by different kinds of loads at the same time. How to effectively analyze and simulate this kind of dynamic environment of structure, named combined dynamic environment, is one of the key issues. In this paper, a novel prediction method of combined dynamic environment is proposed from the perspective of data analysis. First, the existence of dynamic similarity between vibration responses of the same structure under different boundary conditions is theoretically proven. It is further proven that this similarity can be established by a multiple-input multiple-output regression model. Second, two machine learning algorithms, multiple-dimensional support vector machine and extreme learning machine, are introduced to establish this model. To test the effectiveness of this method, shock and stochastic white noise excitations are acted on a cylindrical shell with two clamps to simulate different dynamic environments. The prediction errors on various measuring points are all less than ±3 dB, which shows that the proposed method can predict the structural vibration response under one boundary condition by means of the response under another condition in terms of precision and numerical stability.

1. Introduction

Effective prediction of structural response always plays an important role in the fields of aeronautics, astronautics, car-manufacturing, and so on. One of the key questions is how to accurately analyze and simulate the true dynamic environment of structure. In practical engineering, structures in working condition tend to be excited by different kinds of loads, for example, vibration, shock, noise, overload, and so on, in a synthetic or sequential manner [1, 2]. The dynamic environment constructed by these intricate loads is defined as combined dynamic environment. Structures in bad combined dynamic environment are apt to be broken and the instruments within structures are liable to be invalid. To improve the reliability of structure and instruments, dynamic environmental test is required [3]. However, the existing experimental data for new developed system are scarce, and direct reference from analogous model will cause big error. In order to evaluate structure's reliability and improve structural design, it is necessary to predict the combined dynamic environment and reproduce the true dynamic environment from the beginning of system designing via accurate analysis of various excitation sources [4]. Combined dynamic environment is of significant importance both in theory and in practical engineering.

At present, prediction of dynamic environment includes three major methods: extrapolation method [5, 6], traditional mode method (finite element method) [4], and statistical energy analysis [7]. As a traditional empirical approach, extrapolation method can obtain predictive data directly by means of the statistics of measured data from similar scaling model. However, this kind of method heavily relies on previous experience and is hard to reproduce complex environment. Moreover, it is hard to repeat many times because of high experimental cost. Finite element method and statistical energy analysis have demonstrated impressive performance in predicting structure's vibration environment due to the solid theoretical foundation. Specifically, finite element method is applicable to low-frequency case while statistical energy analysis performs well in middle- and high-frequency areas. However, these two methods still could not handle the uncertainty of combined dynamic environment effectively.

This paper tries to research the prediction of combined dynamic environment from a whole new point of view. The basic idea can be described as follows. In systems composed of a structure and different boundary conditions, the physical property of structure itself is fixed and mainly influences vibration response. The change of structure's dynamic property is only caused by boundary condition's transmissibility, restraint stiffness, and added mass. Therefore, as long as a structure and two different boundary conditions are fixed, there must be a deterministic similarity between two systems' dynamic properties. If this similarity can be modeled from the perspective of data analysis, the response of one system can be evaluated from another system's response, which will provides a new solution for combined dynamic environment prediction.

Based on the above discussions, this paper proposes a novel method of combined dynamic environment prediction, which means predicting the actual response of a structure in combined dynamic environment by means of the response of the same structure in laboratory environment. To the best of our knowledge, there is no previous research applying machine learning methods to combined dynamic environment prediction.

The main contribution of this paper can be summarized as follows.

(i) This paper proves in dynamic theory that there exists a dynamic similarity between the same structure under different boundary conditions.

(ii) This paper proves that this dynamic similarity on multiple measuring points on structure can be viewed as a multiple-input multiple-output (MIMO) regression model.

(iii) This paper proposes a machine learning-based solution for this problem by introducing two efficient machine learning algorithms which are with multiple dimensional outputs.

(iv) This paper constructs a cylindrical shell vibration system to demonstrate that the response of multiple points on a structure with one boundary can be effectively predicted by the response of the same structure with another boundary no matter in what time or frequency domain.

It is worth noting that different machine learning algorithms have various characteristics and performances. The reason of choosing both M-SVR and ELM, rather than only one of them as modeling algorithm, is to remove the potential biased effect of algorithm and get a more accurate and stable result. The rest of this paper is organized as follows. In Section 2, two theoretical proofs about this dynamic similarity relationship are provided. In Section 3, a brief review of extreme machine learning (ELM) and multiple-dimensional support vector regression (M-SVR) is given. Section 4 is devoted to computer experiments where the proposed framework using ELM and M-SVR is evaluated on cylinder stochastic vibration system, followed by a conclusion in the last section.

2. Theoretical Analysis of Mapping Relationship

2.1. Precondition. Generally speaking, a structure constrained with different boundary conditions will construct different dynamic systems and have various dynamic characteristics. According to dynamic theory, model, boundary condition, and load are three key factors to work upon system response. Once the structure has been constrained with boundary condition, there is only load left to influence response due to the fixity of local physical property of boundary condition as well as nature property of structure. Here without loss of generality, the structure and boundary 1 constitute system 1, and the same structure and boundary 2 constitute system 2. Obviously, the only variable factor between these two systems is load. Introducing frequency spectrum of response $y(\omega) = h(\omega)x(\omega)$, if the input is flat spectrum, that is, $x(\omega) = 1$, then $y(\omega) = h(\omega)$. Considering two systems' response $y_1(\omega)$ and $y_2(\omega)$, then we have $y_1(\omega)/y_2(\omega) = h_1(\omega)/h_2(\omega)$, which indicates in this case a similarity relationship exists between two systems' response, and it only depends on intrinsic property of two systems. Based on this analysis, four cognitions, named load equivalent rule, are proposed firstly to shield the extrinsic effect of load as follows.

(i) The geometrical and physical properties (mass, stiffness, damp) of structure remain fixed.

(ii) The differential governing equations of both systems for structural vibration remain identical in form.

(iii) The structure and boundary condition can be viewed as different subsystems of integral system, in which the local property of structure changes as long as restraining stiffness and quality of boundary condition change.

(iv) The restraining stiffness matrix of boundary condition should be nonsingular.

Here, the first three cognitions mean local similarity between two dynamic systems. In short, load equivalent rule is prerequisite to establish the intrinsic dynamic similarity between system 1 and system 2 which is defined as mapping relationship in this paper.

2.2. Existence Proof

Theorem 1. *Suppose that system 1 and system 2 are constructed by the same structure connected with two different boundary conditions. If these two systems meet load equivalent rule, a deterministic regression relationship must exist between the response of the two systems on the same measuring point. This relationship is only relevant to the dynamic parameters of these two systems.*

Proof. This proof will be accomplished by introducing mode analysis and coordinate transformation in time and

frequency domain, respectively. In time domain, the dynamic equations of two systems are as follows:

$$(M + M_1)\ddot{x}_1 + (C + C_1)\dot{x}_1 + (K + K_1)x_1 = f_1(t), \quad (1)$$

$$(M + M_2)\ddot{x}_2 + (C + C_2)\dot{x}_2 + (K + K_2)x_2 = f_2(t), \quad (2)$$

where M, K, and C are structure's mass matrix, stiffness matrix, and damping matrix of order n, M_1, M_2, C_1, C_2, K_1, K_2 denoting the corresponding matrix of fixture 1 and 2, respectively, and $f(t)$ is external load array. From (1) and (2), the following equations are obtained:

$$x_1 = \varphi_1 y_1, \quad (3)$$

$$x_2 = \varphi_2 y_2, \quad (4)$$

where φ_1 and φ_2 are modal matrices of systems 1 and 2 in modal coordinate system I and II, respectively, and y_1 and y_2 are the vectors in corresponding coordinate systems.

From (3) and (4), the relatedness between x_1 and x_2 is implicit. In this paper, coordinate transformation is introduced for decoupling. Due to limitation of space, the concrete procedure of decoupling is omitted here. Without loss of generality, (1) is decoupled as follows:

$$M_{1-2}\ddot{z}_1 + C_{1-2}\dot{z}_1 + K_{1-2}z_1 = \varphi_{1-2}^T \varphi_{1-1}^T f(t), \quad (5)$$

where

$$\begin{aligned} M_{1-2} &= \varphi_{1-2}^T M_1 \varphi_{1-2}, \\ K_{1-2} &= \varphi_{1-2}^T K_1 \varphi_{1-2}, \\ C_{1-2} &= \varphi_{1-2}^T C_1 \varphi_{1-2}, \end{aligned} \quad (6)$$

where φ_{1-2} is modal matrix whose columns are complete orthogonal basis of modal coordinate system II. Note that z_1 is displacement in *z-space* and can be calculated from (5).

Furthermore, according to (3), x_1 can be calculated by the following equation:

$$x_1 = \varphi_{1-1} y_1 = \varphi_{1-1}\varphi_{1-2} z_1 = \varphi_1' z_1. \quad (7)$$

Similarly, x_2 can be obtained as follows:

$$x_2 = \varphi_{2-2} y_1 = \varphi_{2-2}\varphi_{2-1} z_2 = \varphi_2' z_2. \quad (8)$$

By uniting (7) and (8), the solutions are as follows:

$$\begin{aligned} x_{1ij} &= \sum_{k=1}^{n} \varphi_{1ik}' \cdot z_{1kj}, \\ x_{2ij} &= \sum_{k=1}^{n} \varphi_{2ik}' \cdot z_{2kj}. \end{aligned} \quad (9)$$

Therefore, the dynamic relatedness between x_1 and x_2 can be described as follows:

$$x_{1ij} = \frac{\sum_{k=1}^{n} \varphi_{1ik}' \cdot z_{1kj}}{\sum_{k=1}^{n} \varphi_{2ik}' \cdot z_{2kj}} x_{2ij} = \psi_{ij}(t)\, x_{2ij}, \quad (10)$$

where φ_1' and φ_2' are new complete orthogonal basis after coordinate transformation which is irrelevant to external load. From (10), it can be proved that there exists a dynamic similarity between the time domain responses of any two corresponding points in system 1 and 2. Clearly, $\psi_{ij}(t)$ in (10) is a typical regression model between x_{1ij} and x_{2ij}, and more importantly, it only depends on the intrinsic characteristics of two systems.

In a similar way, the existence of this dynamic similarity in frequency domain is also proved. For vibration equation, Laplace Transform is conducted, and under zero initial condition, the relationship between input and output can be described as follows:

$$x(s) = G(s) f(s), \quad (11)$$

where $G(s) = (s^2 M + sC + K)^{-1}$ is transfer function matrix. Without loss of generality, let $s = i\omega$; then the complex frequency response function matrices of system 1 and 2 are as follows:

$$\begin{aligned} x_1(\omega) &= H_1(\omega) f_1(\omega), \\ H_1(\omega) &= \left(K_1 - \omega^2 M_1 + i\omega C_1\right)^{-1}, \\ x_2(\omega) &= H_2(\omega) f_2(\omega), \\ H_2(\omega) &= \left(K_2 - \omega^2 M_2 + i\omega C_2\right)^{-1}. \end{aligned} \quad (12)$$

Supposing that $H_1(\omega)$ and $H_2(\omega)$ are both full rank and $f_1(\omega) = f_2(\omega)$, which obeys load equivalent rule, the following equation can be obtained from (12):

$$x_{1ij}(\omega) = \frac{\sum_{i,j=1}^{n} h_{1ij}(\omega)}{\sum_{i,j}^{n} h_{2ij}(\omega)} x_{2ij}(\omega) = \psi_{ij}(\omega)\, x_{2ij}(\omega). \quad (13)$$

Similar to (10), (13) also indicates that there exists a nonlinear regression relationship in frequency domain between the corresponding nodes of two systems under the same load, and this relationship also depends on the dynamic characteristics of two systems. Therefore, we get the desired conclusion. □

In this paper, this dynamic similarity as shown in (10) and (13) is defined as mapping relationship. Note that the proof of Theorem 1 aims at the case of same measuring point on structure. For different measuring points of two systems, the following lemma is given.

Lemma 2. *Suppose that system 1 and system 2 are constructed by the same structure connected with two different boundary conditions. If these two systems meet load equivalent rule, there is a deterministic regression relationship between the response at different measuring points of the two systems. This relationship only depends on the dynamic parameters of these two systems.*

Proof. Without loss of generality, two measuring points p_1 and p_2 are randomly selected. According to linear system theory, for the same linear system, there is a deterministic

functional relationship $x_{p_1} = g(x_{p_2})$ between the response at p_1 and p_2. Note that the concrete form of functional $g(\cdot)$ only depends on the parameters of the system itself, and there is no need to calculate it. According to Theorem 1, there is a mapping relationship $x_{1p_2} = \psi(x_{2p_2})$ on p_2 between system 1 and system 2. Therefore, a deterministic regression relationship $x_{1p_1} = g(\psi(x_{2p_2}))$ exists between the response at p_1 and the response at p_2, and it is only related to the dynamic parameters of the systems themselves. □

From (10) and (13), the response signals of the two systems perform as the input and output data of mapping model. And according to Lemma 2, the input data on every measuring point influence the output data on all measuring points. Therefore, mapping relationship can be described as an MIMO regression model [8], as shown in Figure 1.

3. Modeling of Mapping

3.1. Machine Learning-Based Solutions. Theoretically speaking, the accurate solution of mapping in (10) and (13) can be calculated after several coordinate transformations. However, modeling mapping is a complex ill-posed problem because the experimental solution of the structural response is generally contaminated by noise, and analytical solution is too hard and computationally expensive to be calculated. From the perspective of data analysis, the model of mapping in Figure 1 can be viewed as a black-box modeling procedure. Considering that the prediction of new structural response is of crucial importance for mapping, machine learning-based method is introduced to establish the mapping model in this paper.

The key issue is to select an efficient and applicable machine learning algorithm for MIMO modeling. The most common way is to disassemble the MIMO model into multiple single-dimensional submodel. In spite of simple implementation, this way is inefficient and cannot utilize the information shared among multiple outputs. For MIMO system, a traditional modeling method is neural network. As a pioneer research, Huang et al. [9] developed an efficient and simple MIMO learning algorithm, called extreme learning machine (ELM), which has its roots in feedforward neural network. When facing sales forecasting and time series prediction problems [10, 11], ELM has shown its benefit in comparison with backpropagation neural networks and support vector machine (SVM). As another excellent MIMO regression tool, Multiple-dimensional support vector regression (M-SVR), proposed by Pérez-Cruz et al. in [12], extends classical SVM to MIMO case by redefining *ε-insensitive* loss function on all outputs. In particular, M-SVR has been applied successfully in the field of channel estimation [13] and can perform well when only scarce samples are available. To test the effectiveness of mapping relationship in Lemma 2, ELM and M-SVR are both introduced to establish the MIMO regression model in Figure 1. The following sections will provide a brief summary of M-SVR and ELM.

3.2. Brief Summary of M-SVR. Given a set of i.i.d. training samples $\{(\mathbf{x}_1, \mathbf{y}_1), \ldots, (\mathbf{x}_n, \mathbf{y}_n)\} \subset \mathbb{R}^d \times \mathbb{R}^Q$, M-SVR is formulated as minimization of the following functional [13]:

$$\min_{\mathbf{W},\mathbf{b}} Lp = \frac{1}{2}\sum_{j=1}^{Q}\left\|\mathbf{w}^j\right\|^2 + C\sum_{i=1}^{n} L\left(u_i\right), \tag{14}$$

where

$$L(u) = \begin{cases} 0 & u < \varepsilon, \\ u^2 - 2u\varepsilon + \varepsilon^2 & u \geq \varepsilon, \end{cases}$$
$$u_i = \left\|\mathbf{e}_i\right\| = \sqrt{\mathbf{e}_i^T \mathbf{e}_i}, \tag{15}$$
$$\mathbf{e}_i^T = \mathbf{y}_i^T - \phi^T(\mathbf{x}_i)\,\mathbf{W} - \mathbf{b}^T,$$
$$\mathbf{W} = \left[\mathbf{w}^1, \ldots, \mathbf{w}^Q\right], \qquad \mathbf{b} = \left[b^1, \ldots, b^Q\right]^T.$$

By adopting the cost function $L(u)$ described in (15), M-SVR is capable of finding the dependencies between outputs and can take advantage of the information of all outputs to get a robust solution. As (14) cannot be solved straightforwardly, an iterative method, named IRWLS, is utilized in [13] to obtain the desired solution. By introducing a first-order Taylor expansion of cost function $L(u)$, the objective of (14) will be approximated by the following equation:

$$Lp'(\mathbf{W}, \mathbf{b}) = \frac{1}{2}\sum_{j=1}^{Q}\left\|\mathbf{w}^j\right\|^2 + \frac{1}{2}\sum_{i=1}^{n} a_i u_i^2 + \mathrm{CT}, \tag{16}$$

where

$$a_i = \begin{cases} 0 & u_i^k < \varepsilon, \\ \dfrac{2C\left(u_i^k - \varepsilon\right)}{u_i^k} & u_i^k \geq \varepsilon, \end{cases} \tag{17}$$

CT is a constant term which does not depend on $\mathbf{W}$ and $\mathbf{b}$, and the superscript k denotes kth iteration.

To optimize (16), an IRWLS procedure is constructed which linearly searched the next step solution along the descending direction based on the previous solution [13]. According to the representer theorem [14], the best solution of minimization of (16) in feature space can be expressed as $\mathbf{w}^j = \sum_i \phi(\mathbf{x}_i)\beta^j = \mathbf{\Phi}^T\boldsymbol{\beta}^j$, so the target of M-SVR is transformed into finding the best $\boldsymbol{\beta}$ and $\mathbf{b}$. The IRWLS of M-SVR can be summarized in the following steps [13].

Step 1. Set $k = 0$, $\boldsymbol{\beta}^k = \mathbf{0}$, $\mathbf{b}^k = \mathbf{0}$. Calculate u_i^k and a_i.

Step 2. Compute the solution $\boldsymbol{\beta}^s$ and $\mathbf{b}^s$ according to the next equation:

$$\begin{bmatrix} \mathbf{K} + \mathbf{D}_a^{-1} & \mathbf{1} \\ \mathbf{a}^T\mathbf{K} & \mathbf{1}^T\mathbf{a} \end{bmatrix} \begin{bmatrix} \boldsymbol{\beta}^j \\ b^j \end{bmatrix} = \begin{bmatrix} \mathbf{y}^j \\ \mathbf{a}^T\mathbf{y}^j \end{bmatrix}, \quad j = 1, \ldots, Q, \tag{18}$$

where $\mathbf{a} = [a_1, \ldots, a_n]^T$, $(\mathbf{D}_a)_{ij} = a_i\delta(i - j)$ and $\mathbf{K}$ is kernel matrix. Define the corresponding descending direction $\mathbf{P}^k = \begin{bmatrix} \mathbf{W}^s - \mathbf{W}^k \\ (\mathbf{b}^s - \mathbf{b}^k)^T \end{bmatrix}$.

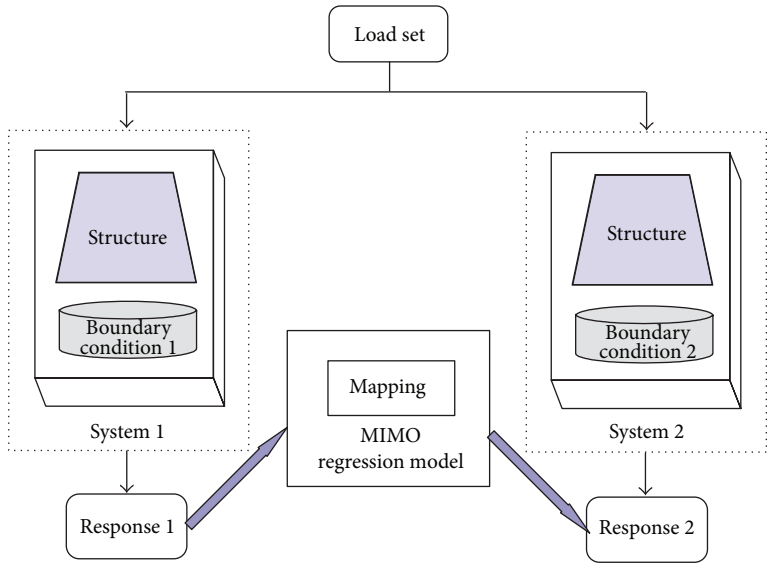

Figure 1: Sketch diagram of mapping relationship between the same structure with different boundary conditions.

Step 3. Use a backtracking algorithm to compute $\boldsymbol{\beta}^{k+1}$ and $\mathbf{b}^{k+1}$ and further obtain u_i^{k+1} and a_i. Go back to Step 2 until convergence.

Once convergence is reached, the jth column of $\boldsymbol{\beta}$ and $\mathbf{b}$ will construct the regressor of jth output. Because u_i^k and a_i are calculated using every dimension of $\mathbf{y}$, each individual regressor contains the information of all outputs, which improves the prediction performance of M-SVR.

3.3. Brief Summary of ELM. As an excellent MIMO regression tool, ELM extends single-hidden layer feedforward neural network (SLFN) to "generalized" hidden node case where its generalization performance and learning speed are both improved than in traditional neural networks. As the theoretical foundations of ELM, [15] studied the learning performance of SLFN on small-size dataset and found that SLFN with at most N hidden neurons can learn N distinct samples with zero error by adopting any bounded nonlinear activation function. Based on this concept, [16] pointed out that ELM can analytically determine the output weights by a simple matrix inversion procedure as soon as the input weights and hidden layer biases are generated randomly and then obtain good generalization performance with very high learning speed.

Given a set of i.i.d. training samples $\{(\mathbf{x}_1, \mathbf{t}_1), \ldots, (\mathbf{x}_N, \mathbf{t}_N)\} \subset \mathbb{R}^n \times \mathbb{R}^m$, standard SLFNs with $\widetilde{N}$ hidden nodes are mathematically formulated as follows [9]:

$$\sum_{i=1}^{\widetilde{N}} \boldsymbol{\beta}_i g_i\left(\mathbf{x}_j\right) = \sum_{i=1}^{\widetilde{N}} \boldsymbol{\beta}_i g_i\left(\mathbf{w}_i \cdot \mathbf{x}_j + b_i\right) = \mathbf{o}_j, \quad j = 1, \ldots, N, \tag{19}$$

where $g(x)$ is the activation function, $\mathbf{w}_i = [w_{i1}, w_{i2}, \ldots, w_{in}]^T$ is input weight vector connecting input nodes and the ith hidden node, $\boldsymbol{\beta}_i = [\beta_{i1}, \beta_{i2}, \ldots, \beta_{im}]^T$ is the output weight vector connecting output nodes and the ith hidden node, and b_i is bias of the ith hidden node. Huang et al. [16] have rigorously proved that then for N arbitrary distinct samples and any $(\mathbf{w}_i, b_i)$ randomly chosen from $\mathbb{R}^n \times \mathbb{R}$ according to any continuous probability distribution, the hidden layer output matrix $\mathbf{H}$ of a standard SLFN with N hidden nodes is invertible and $\|\mathbf{H}\boldsymbol{\beta} - \mathbf{T}\| = 0$ with probability one if the activation function g: $\mathbb{R} \mapsto \mathbb{R}$ is infinitely differentiable in any interval. Then given $(\mathbf{w}_i, b_i)$, training an SLFN equals finding a least-squares solution of the following equation:

$$\mathbf{H}\boldsymbol{\beta} = \mathbf{T}, \tag{20}$$

where

$$\begin{aligned} &\mathbf{H}\left(\mathbf{w}_1, \ldots, \mathbf{w}_{\widetilde{N}}, b_1, \ldots, b_{\widetilde{N}}, \mathbf{x}_1, \ldots, \mathbf{x}_{\widetilde{N}}\right) \\ &\quad = \begin{bmatrix} g\left(\mathbf{w}_1 \cdot \mathbf{x}_1 + b_1\right) & \cdots & g\left(\mathbf{w}_{\widetilde{N}} \cdot \mathbf{x}_1 + b_{\widetilde{N}}\right) \\ \vdots & \cdots & \vdots \\ g\left(\mathbf{w}_1 \cdot \mathbf{x}_N + b_1\right) & \cdots & g\left(\mathbf{w}_{\widetilde{N}} \cdot \mathbf{x}_N + b_{\widetilde{N}}\right) \end{bmatrix}_{N \times \widetilde{N}} \\ &\boldsymbol{\beta} = \left[\boldsymbol{\beta}_1, \ldots, \boldsymbol{\beta}_{\widetilde{N}}\right]^T, \qquad \mathbf{T} = \left[t_1, \ldots, t_{\widetilde{N}}\right]^T. \end{aligned} \tag{21}$$

Considering in most cases that $\widetilde{N} \ll N$, $\boldsymbol{\beta}$ cannot be computed through the direct matrix inversion, therefore, Huang et al. [9] calculated the smallest norm least-squares solution of (20) as follows:

$$\widehat{\boldsymbol{\beta}} = \mathbf{H}^{\dagger}\mathbf{T}, \tag{22}$$

where $\mathbf{H}^{\dagger}$ is the Moore-Penrose generalized inverse of matrix $\mathbf{H}$. Based on the above analysis, Huang et al. [9] proposed ELM whose framework can be stated as follows.

Step 1. Randomly generate input weight and bias $(\mathbf{w}_i, b_i)$, $i = 1, \ldots, \widetilde{N}$.

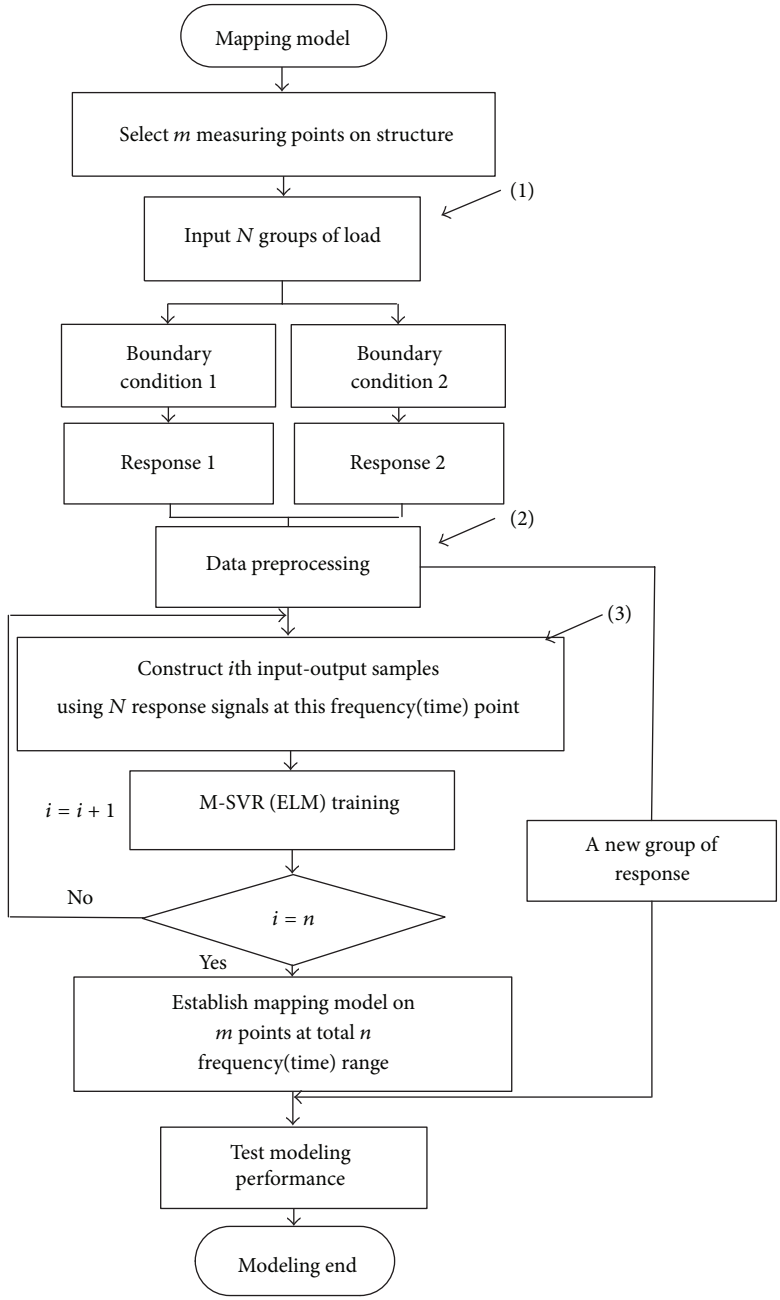

Figure 2: Framework of the proposed prediction method of combined dynamic environment.

Step 2. Compute the hidden layer output matrix $\mathbf{H}$.

Step 3. Compute the output weight $\widehat{\boldsymbol{\beta}} = \mathbf{H}^{\dagger}\mathbf{T}$.

The rigorously theoretical proofs can be found in [17]. Therefore, the output of SLFN can be calculated by $(\mathbf{w}_i, b_i)$ and $\widehat{\boldsymbol{\beta}}$:

$$f\left(\mathbf{x}_j\right) = \sum_{i=1}^{\widetilde{N}} \boldsymbol{\beta}_i g_i\left(\mathbf{w}_i \cdot \mathbf{x}_j + b_i\right). \tag{23}$$

3.4. Modeling Method of Mapping. Based on the MIMO mapping model shown in Figure 1, a novel prediction method of combined dynamic environment is proposed in this section. This method can predict the structural response of a structure with a boundary condition by means of the response of the same structure with another boundary condition. This method can be described as in the following steps.

Step 1. Add a load set on two systems which are composed of the same structure and two different boundary conditions and obtain two groups of different response signals.

Step 2. Reconstruct response signals as input and output samples, respectively, and apply M-SVR (ELM) to training MIMO mapping model.

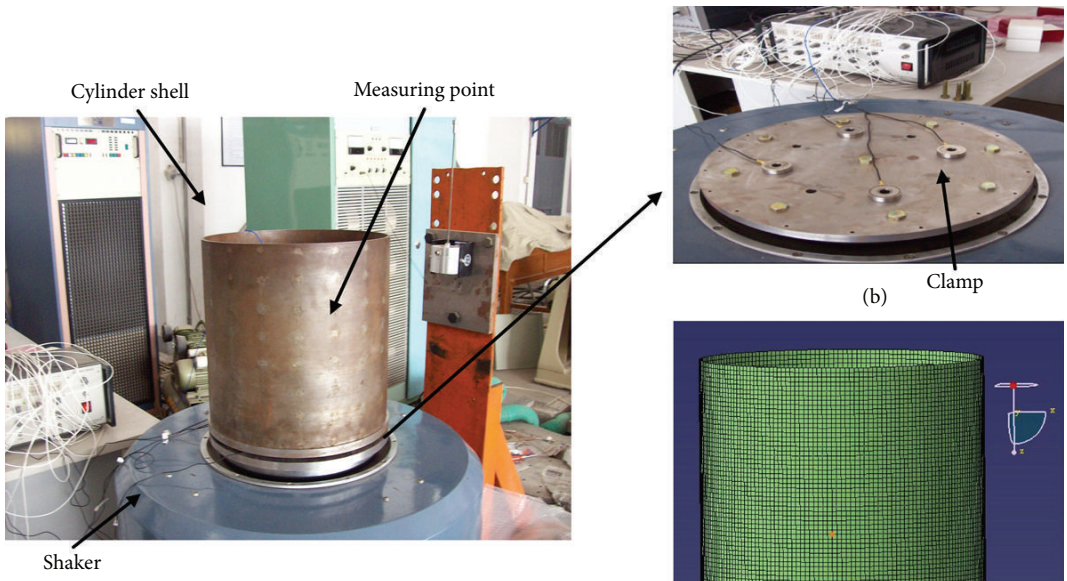

Figure 3: Experimental setup of cylinder stochastic vibration system: (a) cylinder structure assembled on the shaker, (b) a clamp, and (c) finite element model.

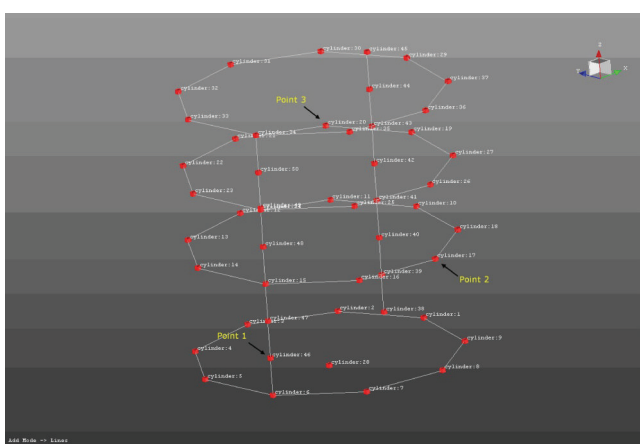

Figure 4: Locations of three accelerometers on cylindrical shell.

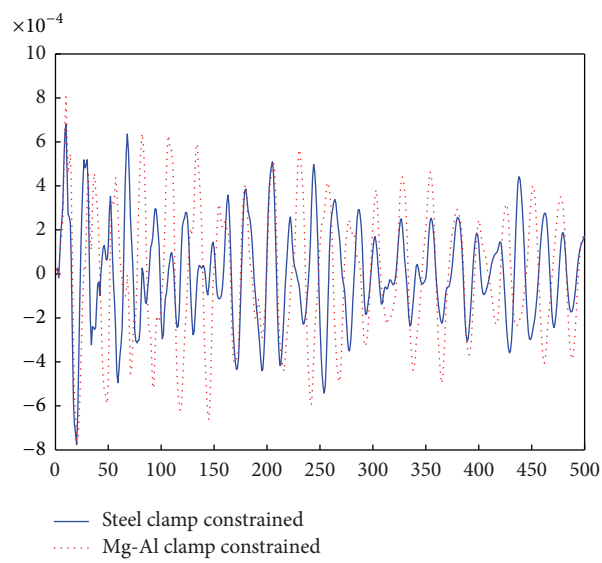

Figure 5: Acceleration responses under two different boundary conditions excited by the same impact load in time domain.

Step 3. Add a new load on one system and use the obtained response signals to predict the response signals excited by the same load in another system.

The key part is using ELM and M-SVR to establish mapping model in an MIMO manner. The reason of applying two machine learning algorithms in this paper is mainly to evaluate the effectiveness of the proposed method more stably while excluding the bias of modeling algorithm. The flow of the proposed method is illustrated in Figure 2.

In Figure 2, there are three marks which need to be explained in detail.

(1) As discussed in Section 2, no matter how the concrete forms of loads vary, the structure itself will not change. Therefore, to establish an accurate mapping model, the data for MIMO training should express intrinsic characteristic of structure effectively. To meet this goal, impact excitation and stochastic white noise are recommended to generate response data for training in this paper.

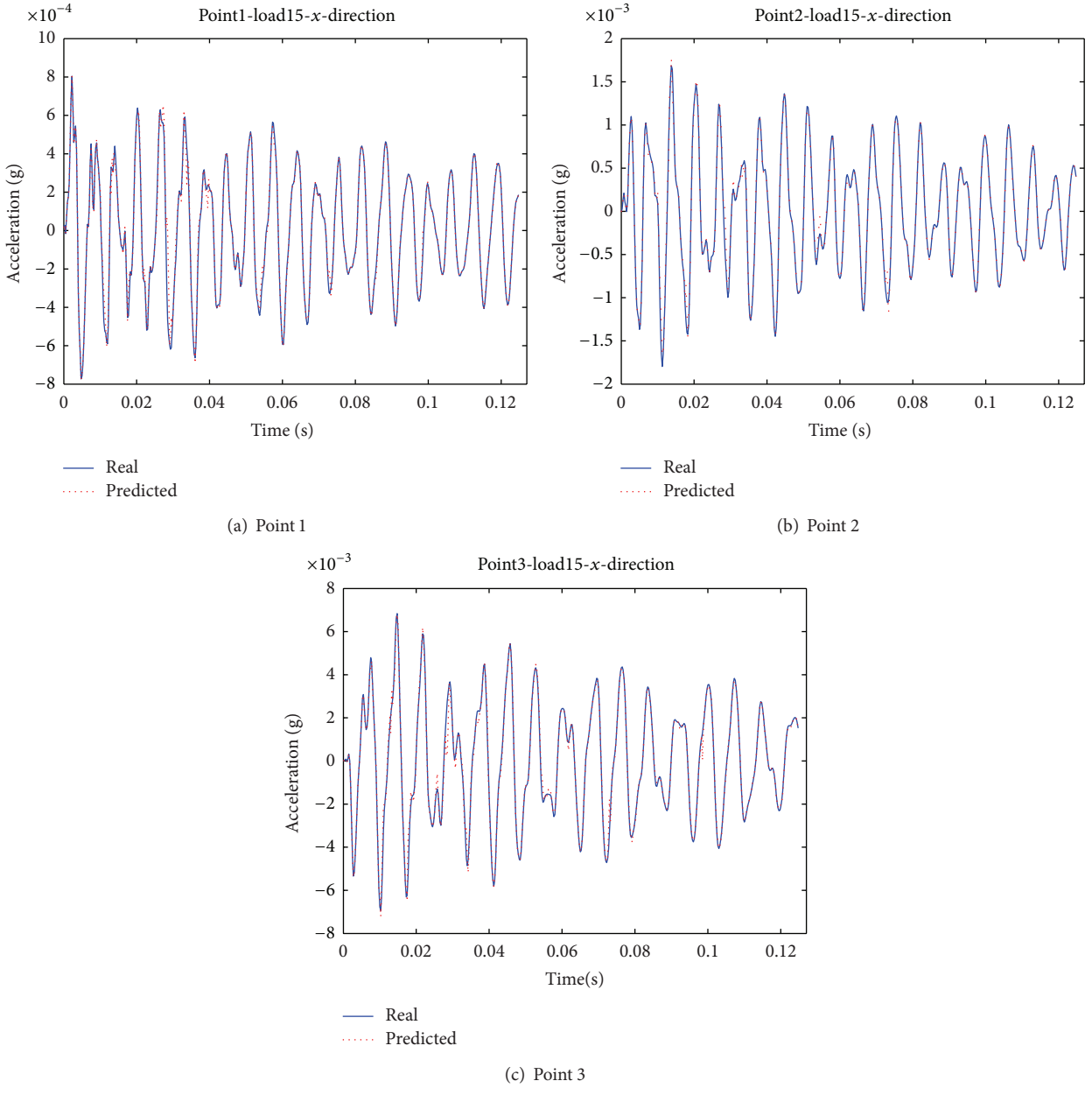

Figure 6: Real and predicted shock acceleration responses of cylindrical shell with Mg-AI clamp by means of response under steel clamp while using M-SVR.

(2) Data preprocessing mainly contains noise reduction for experimental data and extracting features, for example, building frequency data via FFT transformation from time domain.

(3) From (10) and (13), mapping model is established, sampling point by point, in time or frequency domain. Therefore, the sample number equals load number N, and the dimensions of input and output both equal the number of measuring points m. Moreover, considering the order of time series, the data on some previous sampling points can be also introduced to reconstruct training sample as $\hat{x}_i(t) = [x_i(t), x_i(t-1), \ldots, x_i(t-p+1)]$, where p denotes the number of previous points and is called embedding dimension. Here, the input dimension is $m \times p$, and the output dimension is still m.

4. Experiments

As a simplification of many engineering structures, for example, aircraft and car, cylindrical shell is widely used as a typical structure to conduct dynamic environment test. In our previous works [18, 19], a cylindrical shell stochastic vibration system was constructed for study of load identification. In this paper, the same experimental system is used to evaluate the effectiveness of the proposed method. Although the detailed

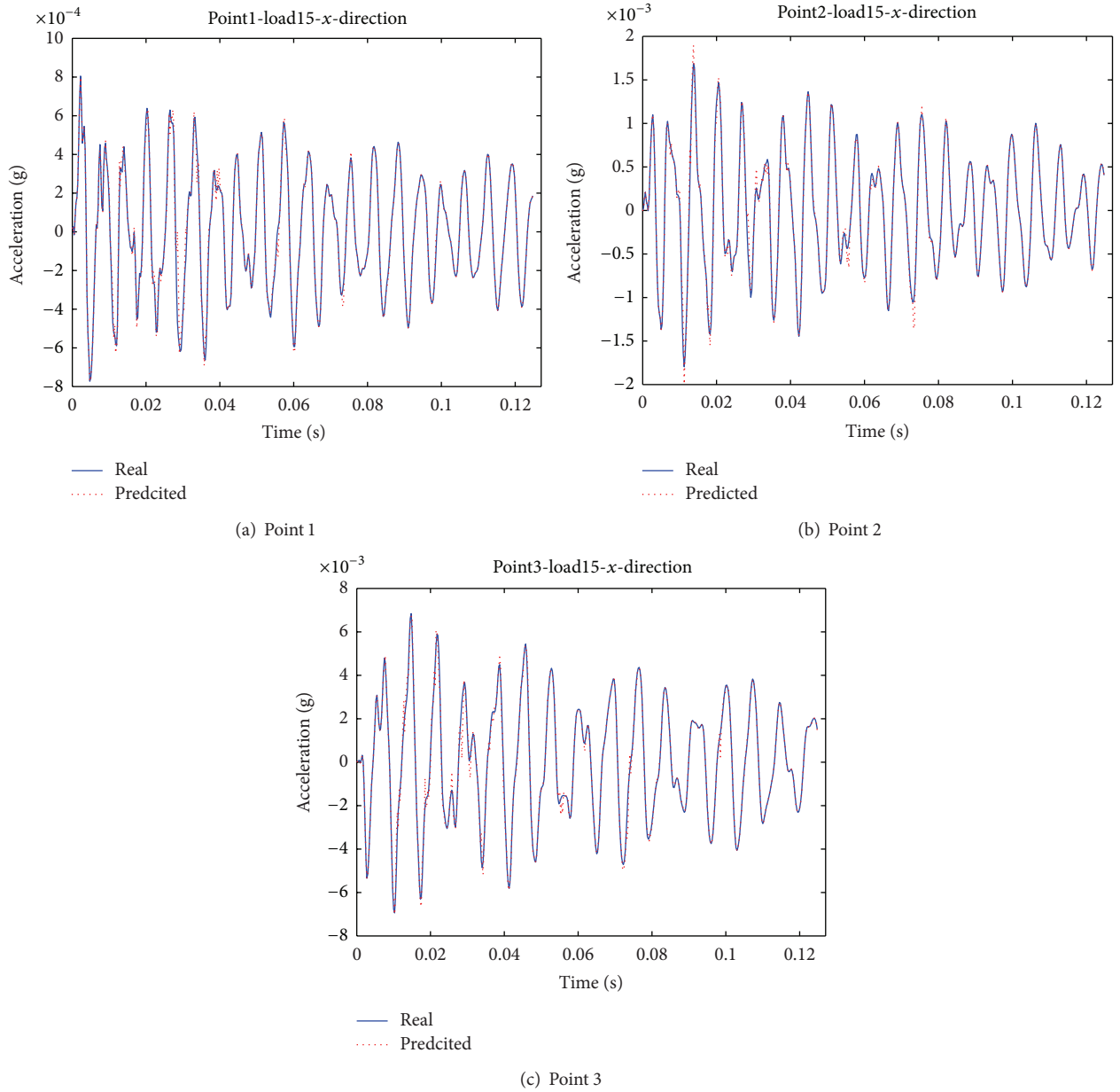

Figure 7: Real and predicted shock acceleration responses of cylindrical shell with Mg-AI clamp by means of response under steel clamp while using ELM.

experimental settings have been described in our previous works, a brief description of this system is also provided for the sake of integrity.

4.1. Data Source. A cylindrical shell made of steel is produced as a researching object. To represent two different boundary conditions, the shell is assembled by steel and magnesium aluminum (Mg-Al) alloy clamps, respectively. In this study, the vibration response of cylindrical shell constrained by Mg-Al clamp (referred to as system 1) is set to predict by the response of cylindrical shell constrained by steel clamp (system 2).

The first issue is to determine the form of external loads. Impact excitation can lead to structure's free vibration in time domain. In frequency domain, if the power spectral density of stochastic excitation is flat spectrum, the corresponding response signals contain all the information of structure's characteristic in whole frequency band. Therefore, to test of mapping modeling, two dynamic datasets, simulation shock response data in time domain, and experimental stochastic response data in frequency domain are generated.

Due to the limitation of the current equipment in our laboratory, instantaneous excitation is hardly to be built. Therefore, finite element models are adopted to generate shock response data. Furthermore, a shaking table stochastic vibration system is also built. The cylindrical shell is assembled by a clamp at the bottom and the whole structure is fixed on a shaking table by 4 bolts. The whole cylindrical shell stochastic vibration system is plotted in Figure 3.

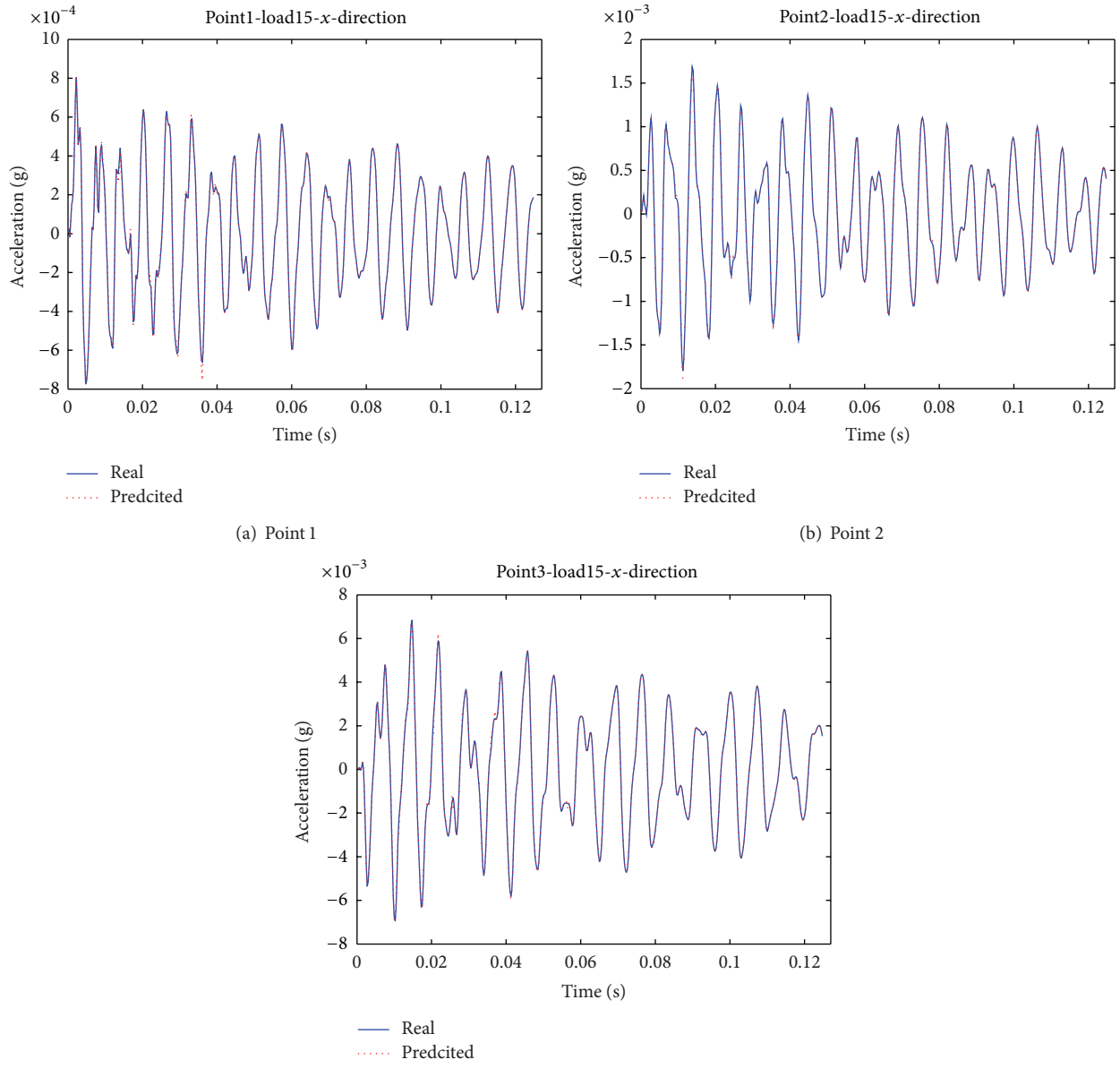

Figure 8: Real and predicted shock acceleration responses of cylindrical shell with embedding dimension is 2.

In Figure 3, the physical characteristics of cylindrical shell and two clamps can be found in [20]. To verify the natural frequency and vibration mode determined by finite element method, it is necessary to conduct modal impact test using impact hammer excitation in advance. The results in [20] show that the first eight natural frequencies of two clamps differ greatly, which means that their dynamic properties are quite different.

The surfaces of structure are placed 144 measuring points in 8 turns. At the "+" mark in Figure 3(c), 30 groups of half a sine pulse loads are acted in radial direction. To get various forms of load, the pulse width is set from 1ms to 15.5 ms with the interval of 0.5 ms. Finally, 30 groups of simulated acceleration response signals in time domain are collected in X, Y, and Z directions. For stochastic vibration test, totally 30 groups of stochastic loads (drive currents) with various spectrum patterns are input to drive shaking table. Acceleration sensors are adopted to collect response signals. Correspondingly, 30 groups of acceleration signals in axial direction are recorded by LMS Test.Lab and further transformed into the power spectral densities (PSD) with sampling frequency of 4096 Hz and frequency interval of 1 Hz. Maximum entropy spectral estimation method is utilized to denoise and smooth the signals. Note that the noise in the collected data will inevitably decrease the prediction performance.

4.2. Simulated Shock Data in Time Domain. Due to the limitation of paper's space, only three measuring points are chosen to conduct mapping modeling, as shown in Figure 4.

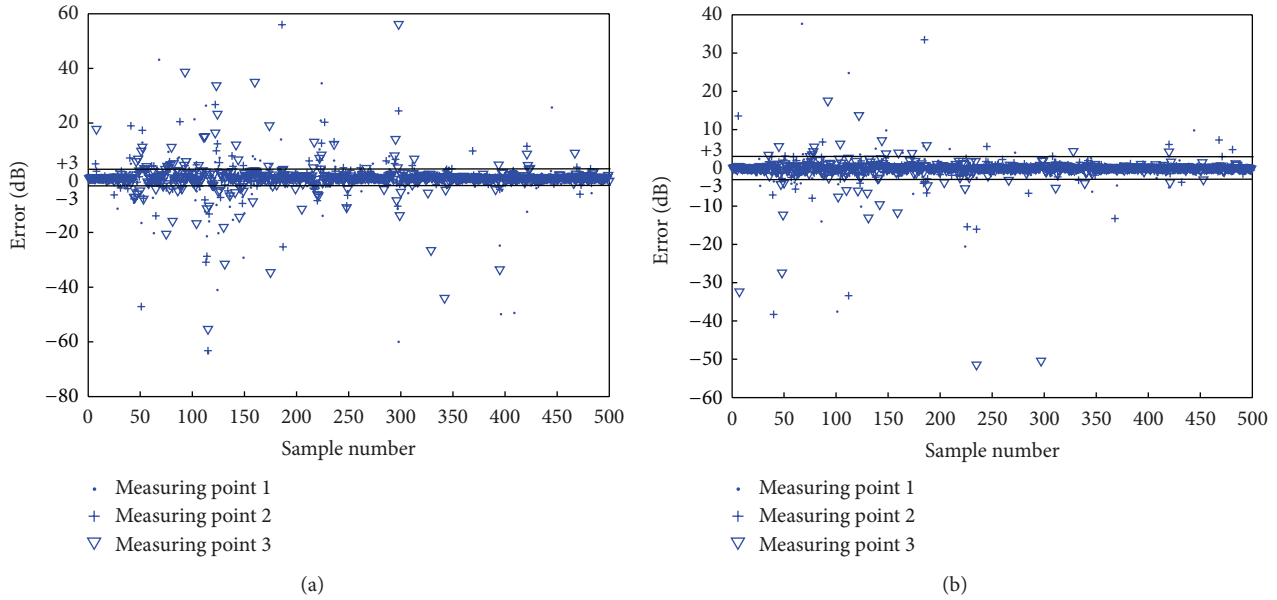

Figure 9: Decibels errors on three measuring points in (a) Figure 7 and (b) Figure 8.

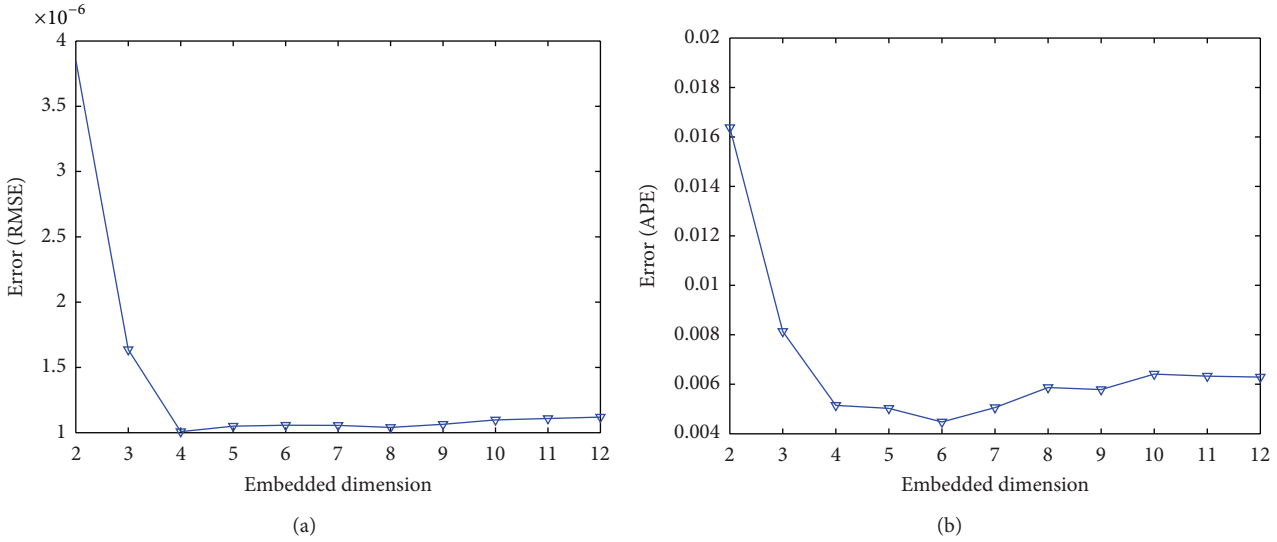

Figure 10: Prediction errors with respect to different embedding dimensions in terms of (a) RMSE and (b) APE.

Firstly, choosing a group of load randomly, Figure 5 gives the comparison of two systems' acceleration response on point 1 in Figure 4. Obviously, there is a large difference between the response of the systems under different boundary conditions, which appears in amplitude and peak values.

The 15th group of response signal in total 30 groups is randomly chosen for prediction. The rest 29 groups of response are used for training. The target of this research is to predict the response under Mg-AI clamp from the response under steel clamp. The prediction performances on three points using M-SVR and ELM are shown in Figures 6 and 7, respectively. The regularization parameter C is set to 100. RBF kernel is adopted and the parameter σ is set to 2. Epsilon is set to 0.001. The number of the hidden neurons is set to 10.

Obviously, M-SVR and ELM both get satisfactory prediction performance on three measuring points at most time points. Particularly at peaks, the predicted values are almost close to the real values. The results demonstrate the effectiveness of the proposed method in time domain. From the perspective of data analysis, because multiple outputs (measuring points) relate closely to each other, M-SVR and ELM are very applicable to improving the prediction performance by exploiting the information shared among outputs. Note that, although simulation data do not contain any noise, there are still some deviations at some time points. It is because of the shortage of information contained at single time point in a time series. To solve this problem, it needs to reconstruct training samples for increasing information

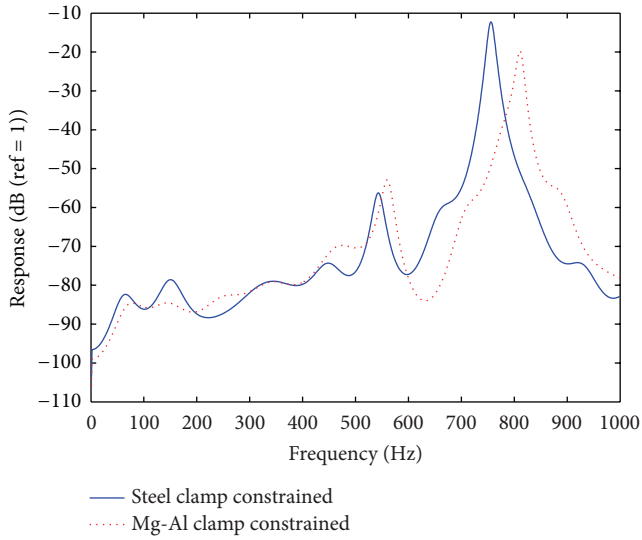

Figure 11: PSDs of cylindrical shell under two different boundary conditions.

through importing some previous time points. As stated in Section 3.4, the number of these time points is called embedding dimension which is a technical term in time series prediction. Defining embedding dimension $p = 2$, that is, adding the nearest time point in training sample, the improving performance is illustrated in Figure 8. Here ELM is used for modeling.

Comparing Figures 7 and 8, merely adding a time point in training sample, most of original deviations at peaks in Figure 7 are decreased in Figure 8. From the perspective of quantitative analysis, Figure 9 gives decibel errors on three measuring points in Figures 7 and 8, respectively.

It is well known that ±3 dB is a widely used limit of experimental error in practical vibration engineering. In Figure 9, ±3 dB is designated by two horizontal lines, and obviously, the errors of most time points are within the limit of ±3 dB. Particularly after introducing embedding dimension, the values of maximum error and the number of time points whose error is out of range ±3 dB both decrease remarkably in Figure 9(b). Taking measuring point 1 as an example, there are 17.4% time points whose error exceeds ±3 dB in Figure 9(a), and its RMSE value is $4.06e-5$ while the average percentage error (APE) is 14.5%. In Figure 9(b), after setting embedding dimension as 2, the corresponding values are 5.8%, $1.25e-5$, and 6.72%, respectively, where the last two values have fallen to 69.2% and 53.7%. Other two measuring points have similar performance.

In addition, it is necessary to determine the proper embedding dimension. Figure 10 provides variation trend of prediction error with respect to different embedding dimensions. ELM is adopted as a modeling algorithm. All features in training sample have been linearly recalled into $[-1, 1]$.

From Figure 10, two errors both decrease remarkably as soon as embedding dimension increases at initial stage. After the minimums occur at 4 and 6, respectively, the errors bounce back slightly. The reason is that mapping model will express dynamic property of systems more accurately if the data of some neighboring time points can be imported into training samples. However, adding too much response data will inversely cause information redundancy which can decrease prediction performance. Particularly speaking, redundant features perhaps lead to more errors when calculating the generalized inverse matrix in ELM. Therefore, it is very important to determine the proper embedding dimension in advance for mapping modeling in time domain.

Finally, computational costs of the above experiments are tested. All programs are carried out in MATLAB2010a environment running in a Core 2, 2.66 GHz CPU, and 3.37 GB RAM. Computation time of experiment using M-SVR (Figure 6) is 5.857 s, while the time using ELM (Figure 7) is 2.385 s. All experiments need less time even though embedding dimension has been introduced. It is because that MIMO structure avoids training on each measuring point repeatedly, and IRWLS procedure in M-SVR is rapid while ELM merely needs calculating a generalized inverse matrix.

4.3. Experimental Stochastic Data in Frequency Domain. In this section, the experimental settings and parameters of M-SVR and ELM are exactly identical to those in the above section. Firstly, selecting a group of load randomly, Figure 11 shows the PSD values under two different boundary conditions on measuring point 1. Similar to the case in time domain, there is also a large difference between the responses of two systems, especially at main peak.

The response of the 10th group of load is randomly chosen for predict, and the responses of other 29 groups of loads are used for training. The prediction results using M-SVR and ELM are illustrated in Figures 12 and 13, respectively.

Obviously, the prediction curves using M-SVR and ELM are both close to the real curve on three measuring points, especially at main peak. The results demonstrate the effectiveness of the proposed method in frequency domain. Note that, looking intuitionisticly from Figures 12 and 13, the prediction performance in this experiment is less than the performance in time domain. It is because that this experiment uses experimental data which inevitably contain measurement error and noise while the experiment in time domain uses simulation data which are free of noise. Although Burg method is adopted for noise reduction, the actual data still have much randomness, which results in less information for representing the model accurately through 29 training samples. Therefore, relativly bigger errors are inevitable. The numerical results using M-SVR and ELM are listed in Table 1.

In Table 1, outlier is denoted as the percentage of time points whose error is out of range ±3 dB in total sampling points. Similar to Figures 12 and 13, the prediction errors using experimental data in frequency domain are larger than the errors using simulation data in time domain. Note that the errors on measuring point 1 are larger than those on the other two points, which is caused by the nearer distance of point 1 from shaking table and resulting stronger noise. Moreover, the experiments using M-SVR (Figure 12) take time 6.313 s, while the time using ELM (Figure 13) is 2.665 s. Therefore,

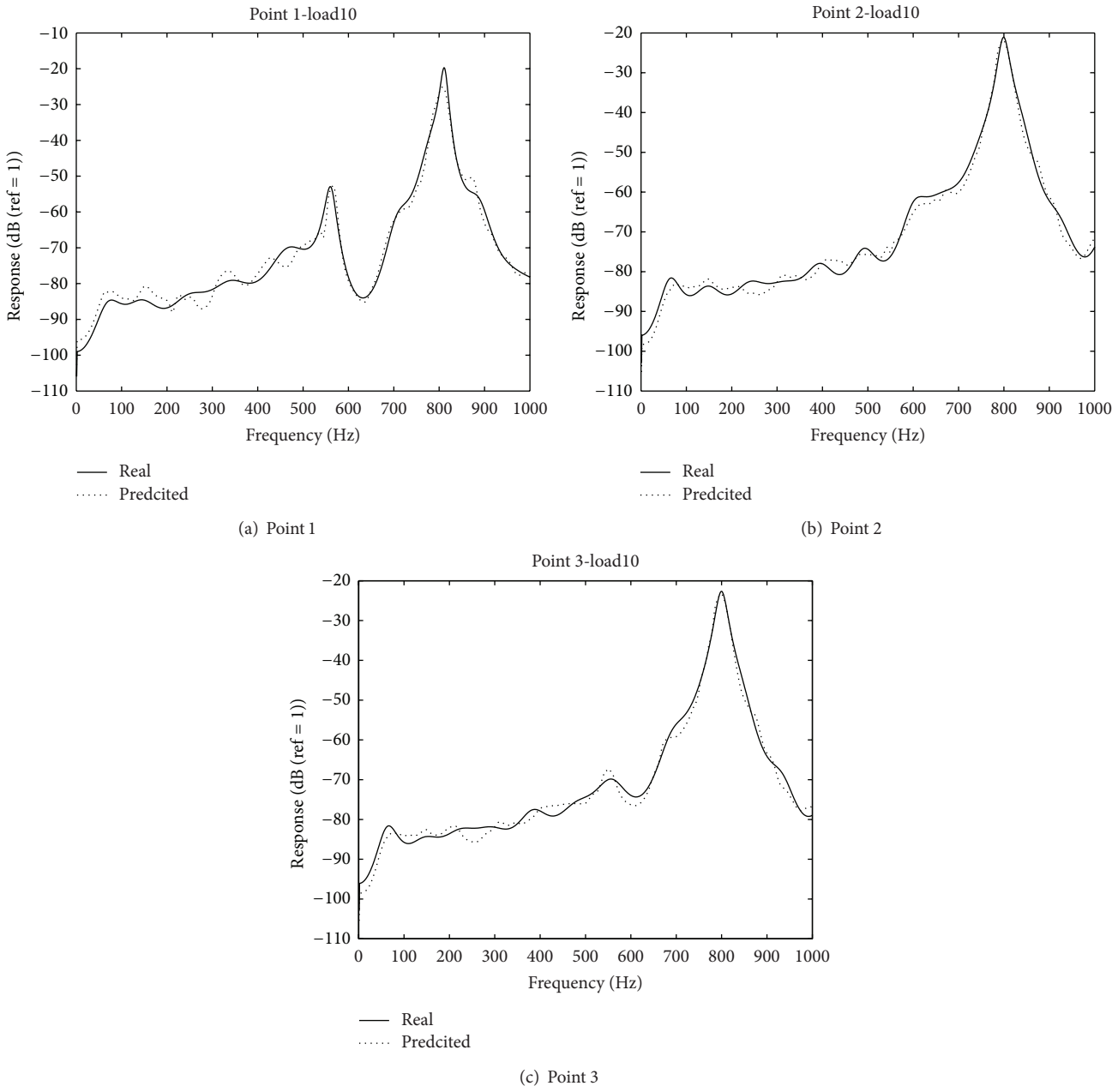

Figure 12: Real and predicted PSD of cylindrical shell with Mg-AI clamp by means of responses under steel clamp while using M-SVR.

no matter from prediction accuracy or computational time both can prove the effectiveness of the proposed method in frequency domain.

To evaluate the performance of the proposed method more convincingly, the prediction errors of total 144 measuring points on whole shell are also tested, as listed in Table 2.

Obviously, MSVR and ELM both get similar predictive performance on total points. Three error indices of two algorithms are all low, which demonstrates that the proposed machine learning-based method works effectively. It is worth noting that the signals near the shell's bottom have larger noise than other parts in stochastic vibration. Therefore, the whole prediction errors are relatively increased.

5. Conclusion

This research is a completely new attempt to apply machine learning algorithms to solving the problem of combined dynamic environment prediction. This paper firstly proves in dynamic theory that a mapping relationship exists between the response signals of the same structure with different boundary conditions and further proves that it is essential to use an MIMO regression model on different measuring points. Based on these theoretical proofs, two machine learning algorithms, M-SVR and ELM which both have MIMO structure and are applicable to small-scale sample problem, are introduced to establish mapping model. Then

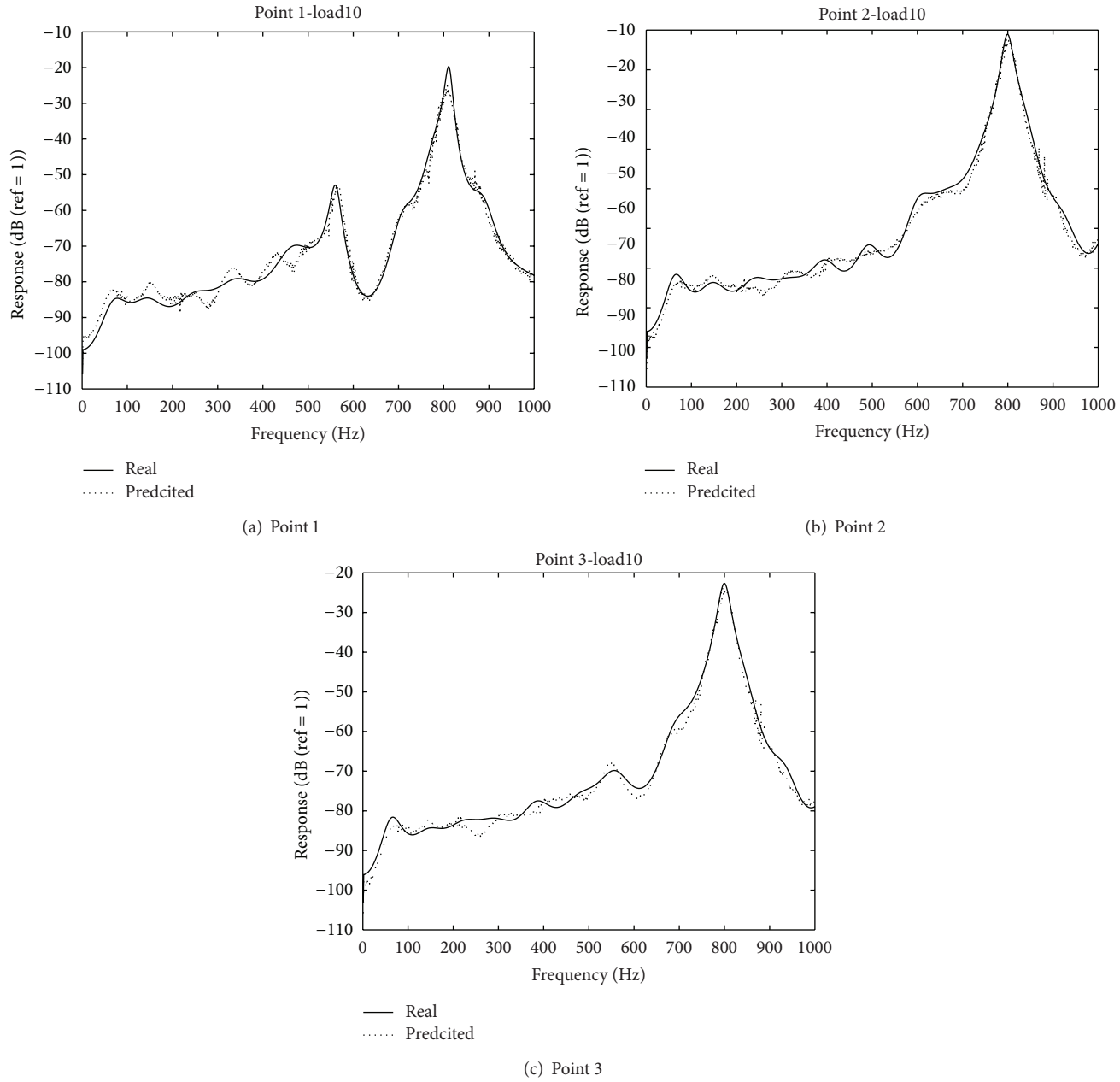

Figure 13: Real and predicted PSD of cylindrical shell with Mg-AI clamp by means of responses under steel clamp while using ELM.

Table 1: Prediction errors of cylindrical shell stochastic vibration experiments in frequency domain.

	Measuring point 1		Measuring point 2		Measuring point 3	
	MSVR	ELM	MSVR	ELM	MSVR	ELM
RMSE	0.0058	0.0068	0.0020	0.0027	0.0015	0.0023
APE (%)	19.96	19.69	16.03	15.38	15.57	14.77
Outlier (%)	21.9%	22.4%	9.9%	9.5%	10.8%	9.7%

a novel prediction method for combined environment is proposed to predict the response of a structure under one boundary condition by means of the response of the same structure under another boundary condition. This research provides a new solution for prediction of combined dynamic environment, which means using the vibration response in laboratory environment to establish mapping model and further predict the real response in working environment, and finally calculating (predicting) the real load by means of the predicted response. Referring to the predicted load,

Table 2: Mean prediction errors and their standard deviation (in bracket) of whole measuring points on cylindrical shell.

	Simulation shock data		Experimental stochastic data	
	MSVR	ELM	MSVR	ELM
RMSE	$4.31e-5$ ($2.60e-5$)	$5.68e-5$ ($2.06e-5$)	0.0068 (0.0033)	0.0076 (0.0041)
APE (%)	13.82 (3.50)	15.02 (4.34)	21.51 (5.92)	23.37 (5.20)
Outlier (%)	12.54%	12.98%	14.53%	16.34%

more reasonable environment conditions and test standards can be effectively laid down to reduce test cost and improve structural design.

An advantage of this research is establishing mapping model on multiple measuring points on structure with high precision and very little computational time. MIMO model of mapping is in accordance with engineering requirement and direct-viewing understanding. Moreover, it can also get lower prediction error than modeling on single point via adding model's information by exploiting the dependency among all outputs. Numerical results using these two algorithms demonstrate the benefit of the proposed method. Note that due to the limitation of our experimental equipment, only 30 groups of response are collected. That means the mapping that modeling in this paper is a typical machine learning problem with small-scale samples. The future work will be going on at the following aspects: (1) enhancing experimental capability and generating more valid response data; (2) calculating the theoretical solution of typical structure; and (3) developing model selection method of M-SVR and ELM for better generalization performance on small-scale sample problems.

Acknowledgments

This work was supported by the National Natural Science Foundation of China (U1204609) and Foundation and Advanced Technology Research Program of Henan Province, China (no. 122300410111).

References

[1] R. L. Barnoski, A. G. Piersol, W. F. van der Laan et al., "Summary of random vibration prediction procedures," NASA CR-1302, 1969.

[2] R. E. Barrett, "Techniques for predicting localized vibratory environments of rocket vehicles," NASA TN-l836, 1963.

[3] P. A. Franken, "Sound-induced vibrations of cylindrical vehicles," *Journal of the Acoustical Society of America*, vol. 34, no. 4, pp. 453–454, 1962.

[4] E. Szücs, *Similitude and Modeling*, Elsevier Scientific Publishing Co., New York, NY, USA, 1980.

[5] P. Singhatanadgid and A. Na Songkhla, "An experimental investigation into the use of scaling laws for predicting vibration responses of rectangular thin plates," *Journal of Sound and Vibration*, vol. 311, no. 1-2, pp. 314–327, 2008.

[6] J. Rezaeepazhand, G. J. Simitses, and J. H. Starnes, "Design of scaled down models for predicting shell vibration response," *Journal of Sound and Vibration*, vol. 195, no. 2, pp. 301–311, 1996.

[7] R. H. Lyon and R. G. De Jong, *Theory and Applications of Statistical Energy Analysis*, Butterworth-Heinemann, Boston, Mass, USA, 1995.

[8] C. M. Bishop, *Pattern Recognition and Machine Learning*, Springer, New York, NY, USA, 2006.

[9] G. B. Huang, Q. Y. Zhu, and C. K. Siew, "Extreme learning machine: theory and applications," *Neurocomputing*, vol. 70, no. 1–3, pp. 489–501, 2006.

[10] F. L. Chen and T. Y. Ou, "Sales forecasting system based on Gray extreme learning machine with Taguchi method in retail industry," *Expert Systems with Applications*, vol. 38, no. 3, pp. 1336–1345, 2011.

[11] X. Zhang and H. L. Wang, "Selective forgetting extreme learning machine and its application to time series prediction," *Acta Physica Sinica*, vol. 60, no. 8, Article ID 080504, 2011 (Chinese).

[12] F. Pérez-Cruz, G. Camps-Valls, E. Soria-Olivas et al., "Multi-dimensional function approximation and regression estimation," *Lecture Notes in Computer Science*, vol. 2415/2002, pp. 757–762, 2002.

[13] M. Sánchez-Fernández, M. de-Prado-Cumplido, J. Arenas-García, and F. Pérez-Cruz, "SVM multiregression for nonlinear channel estimation in multiple-input multiple-output systems," *IEEE Transactions on Signal Processing*, vol. 52, no. 8, pp. 2298–2307, 2004.

[14] B. Schölkopf and A. J. Smola, *Learning with Kernels*, MIT Press, 2002.

[15] G. B. Huang and H. A. Babri, "Upper bounds on the number of hidden neurons in feedforward networks with arbitrary bounded nonlinear activation functions," *IEEE Transactions on Neural Networks*, vol. 9, no. 1, pp. 224–229, 1998.

[16] G. B. Huang, L. Chen, and C. K. Siew, "Universal approximation using incremental constructive feedforward networks with random hidden nodes," *IEEE Transactions on Neural Networks*, vol. 17, no. 4, pp. 879–892, 2006.

[17] G. B. Huang, D. H. Wang, and Y. Lan, "Extreme learning machines: a survey," *International Journal of Machine Learning and Cybernetics*, vol. 2, no. 2, pp. 107–122, 2011.

[18] W. Mao, D. Hu, and G. Yan, "A new SVM regression approach for mechanical load identification," *International Journal of Applied Electromagnetics and Mechanics*, vol. 33, no. 3-4, pp. 1001–1008, 2010.

[19] D. K. Hu, W. T. Mao, J. Zhao, and G. R. Yan, "Application of LSSVM-PSO to load identification in frequency domain," in *Proceedings of Artificial Intelligence and Computational Intelligence*, pp. 231–240, Shanghai, China, 2009.

[20] D. K. Hu, F. Han, and G. R. Yan, "Modeling on the cylindrical shell vibration test system," in *Proceedings of the LMS China User Conference*, Xi'an, China, 2008.